Materials Science Forum Vols 638-642 (2010) pp 1500-1505 *Online: 2010-01-12*
© (2010) Trans Tech Publications, Switzerland
doi:10.4028/www.scientific.net/MSF.638-642.1500

Friction stir welding of SiCp/Al composite and 2024 Al alloy

B.L. Xiao[1, a], D. Wang[1, b], J. Bi[1, c], Z. Zhang[1, d], Z.Y. Ma[1, e]

[1]Shenyang National Laboratory for Materials Science, Institute of Metal Research, Chinese Academy of Sciences, 72 Wenhua Road, Shenyang 110016, China

[a]blxiao@imr.ac.cn, [b]dongwang@imr.ac.cn, [c]jbi@imr.ac.cn, [d]zzhang@imr.ac.cn, [e]zyma@imr.ac.cn

Keywords: Friction stir welding; metal-matrix composites; aluminum; fracture

Abstract. 6 mm thick SiCp/2009Al composite and 2024Al-T351 alloy plates were successfully joined by friction stir welding (FSW) with and without the tool pin offsetting to the 2024Al side (denoted as NOS and OS samples, respectively), producing defect-free joints. The SiC particles from the composite were distributed along a ring structure in the nugget and the volume fraction of the SiC particles decreased as the tool pin offset to the 2024Al side. The Al-clad layer on the 2024Al plate was aggregated on the retreating side of the nugget after FSW. For the OS sample, the Al formed a layer along the nugget boundary. The strength of the NOS sample reached up to 85% of the 2024Al alloy with the joint failing in the heat affected zone on the 2024Al side. The strength of the OS samples was 47% of the 2024Al alloy due to the aggregated Al layer on the retreating side of the nugget which decreased the strength of the joint.

Introduction

Wide industrial applications of the metal-matrix composites (MMCs) depend on effective joining methods such as solid state and fusion processes, which are still specific material and process dependent. It is hard to achieve defect-free welds by using conventional fusion welding techniques [1]. The drawbacks such as the incomplete mixing of the parent and filler materials, eutectic formation and the presence of porosity in the fusion zone limited the joining of the MMCs by fusion welding. In this case, the solid state welding techniques are highly desirable.

Friction stir welding (FSW) is a novel solid-state welding method, particularly applied in aerospace and automotive industries. In the welding process, localized heating, resulted from friction between the tool and workpieces, softens the material around the pin, and the combination of tool rotation and translation results in movement of material from the front to the back of the pin, thereby producing a welded joint in solid state [2]. Therefore, FSW is considered a promising welding technique for joining the MMCs to avoid the drawbacks of the fusion welding. In the last few years, a number of investigations have been conducted to join the aluminum matrix composites by FSW [3-5]. It is indicated that high-quality FSW composite joints could be achieved under optimized parameters. Successful joining of the MMCs will be beneficial to promoting the practical applications of the MMCs.

On the other hand, as advanced structural materials, it is inevitable that the MMCs are joined to other metallic materials. Therefore, successfully joining of the MMCs to the commercial alloys is of practical importance for broadening the applications of the MMCs. Similar to the welding of the MMCs, the fusion welding technique has been proved to be not feasible due to the existence of various welding defects in case of welding of MMCs to the commercial alloys. Therefore, it is necessary to explore the feasibility of joining the composites to the unreinforced alloys by FSW.

Wert reported the first result for FSW between 20vol.%Al_2O_3/2014Al composite and 2024Al alloy [6]. While the microstructural evolution during FSW was subjected to a detailed examination, no mechanical properties of the joint were reported [6]. Recently, Fuchs et al. [7] investigated the FSW of 25vol.%SiCp/2124Al composite to 2024Al alloy. The strength of the joints reached up to 77% of the 2024Al base metal (BM).

It is noted that the studies on the welding of the MMCs to the commercial alloys are quite limited so far. Therefore, it is worthwhile to further investigate the weldability between the MMCs and commercial alloys under various welding conditions. In this paper, 15vol.%SiCp/2009Al composite and 2024Al alloy plates were subjected to FSW with and without the tool offset. The aim is to investigate the effect of welding conditions on the microstructure and mechanical properties of the joints.

Experimental

6 mm thick plates of 15vol.%SiCp/2009Al MMC and Al-clad 2024Al-T351 alloy with a composition of Al-4.2Cu-1.56Mg-0.61Mn-0.1Si-0.15Fe (wt.%) were friction stir butt welded, with and without tool pin offset to the 2024Al side, at a welding speed of 100 mm/min and a tool rotation rate of 800 rpm. The MMC was put on the advance side and the 2024 alloy on the retreating side. OS and NOS referred to the samples welded with the offset (87.5% of pin in the 2024Al side) and without that, respectively. A tool with a shoulder 20 mm in diameter and a cylindrical pin 8 mm in diameter and 5.8 mm in length was used. The MMC was solution treated at 516^{o}C for 1 h and then quenched into water at room temperature. The welding was performed in 1h after quenching. After welding, the joints were naturally aged for 7 days.

The joints were cross-sectioned perpendicular to the welding direction for optical microscopic (OM) examination and hardness measurement. The OM specimens were mechanically polished and etched by a solution of HF 1 ml, HCl 1.5 ml, HNO_3 2.5 ml, H_2O 195 ml. The Vickers hardness profiles of the welds were measured on the cross section along the center line of the welded plates. Dog-bone shaped tensile specimens with a gauge length of 40 mm and a width of 10 mm were machined perpendicular to the welding direction with the nugget zone (NZ) being in the center of the gauge. The fracture surfaces of the tensile specimens were observed by the scanning electron microscopy (SEM).

Results and discussion

Fig. 1a shows the typical cross-sectional macrograph of the NOS sample. No defects were detected in the joint, indicating that the sound joining was achieved between the MMC and 2024Al alloy by FSW. Apparent rings were observed in the NZ. The optical examination shows the gray and grayish rings in the NZ corresponded to SiC particle-rich and -deficiency bands. Similar phenomenon has been previously reported [6]. Chen et al. [8] reported that in the FSW process of Al alloys, the thread of the tool pin sheared material from the matrix and the material in a thread space was spread into a layer as a result of the equivalent downward motion of the thread flank, thereby forming the banded structures in the NZ. Therefore, the ring structure in this study is attributed to alternate disposition of the MMC and 2024Al layers sheared from two sides by the thread of tool pin. Some pure Al (denoted by A in Fig. 1a) was observed in the bottom of the thermo-mechanically affected zone (TMAZ) on the retreating side, which was the Al-clad layer of the 2024Al aggregated on the retreating side during FSW. Some pure Al, the white zone, was also present in the bottom of the NZ.

Similar macrostructure was also observed in the OS sample, shown in Fig. 1b. However, more Al aggregated on the retreating side and formed a layer on the edge of the NZ on the retreating side (as shown by B in Fig. 1b). Some researchers [8,9] reported that the thread on the pin sheared the materials and made the materials flow to the bottom of the plate during the FSW process. On the retreating side, when the materials at the edge of the NZ moved to the bottom, the aggregated Al on the retreating side would move to the middle of the plate. For the OS sample, more 2024Al alloy was in the NZ. Therefore, there was more Al on the retreating side. These Al flowed to the middle of the plate along the edge of the nugget and formed a layer of Al.

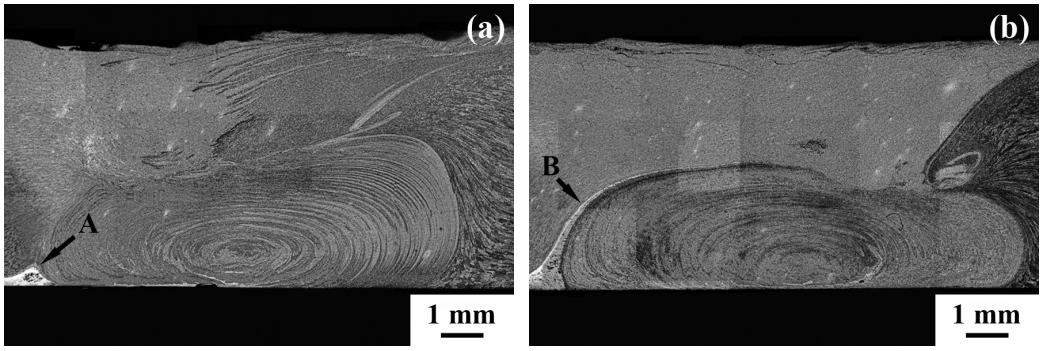

Figure 1. Optical micrographs showing NZ of FSW MMC and 2024Al alloy: (a) NOS sample, (b) OS sample (the advancing side is on the right).

Fig. 2a illustrates the optical microstructure of the SiC/2009Al composite. The SiC particles were distributed along the rolling direction. After FSW, for the NOS sample, because of the mixing of the MMC and 2024Al alloy, the fraction of the SiC particles decreased compared to the original MMC sample (Fig. 2b, the center of the NZ). For the OS sample (Fig. 2c, the advancing side of the NZ), the fraction of the SiC particles was lower compared to the OS samples because less MMC was stirred into the NZ.

Fig. 3 illustrates the hardness profiles of both the NOS and OS samples. The zero point denotes the center of the NZ and the distance from the zero indicates the interval from the tested point to the center of the nugget. For the FSW MMC-2024Al samples, the hardness profiles are quite different from that for the FSW 2024Al joint [10]. For the FSW 2024Al alloy, the heat-affected zone (HAZ) exhibited the lowest hardness due to the coarsening and dissolution of the strengthening precipitates, whereas the hardness of the NZ was lower than that of the BM due to the fundamental dissolution of the precipitates. For the NOS sample, on the retreating side (RS, 2024Al side), similar to the FSW 2024Al alloy, the HAZ had the lowest hardness, however, the hardness of the NZ on the RS was almost equal to that of the 2024Al BM because some SiC particles were stirred into the NZ, which increased the hardness of the NZ. On the advancing side (AS), the hardness profiles are similar to those on the RS with the HAZ having the lowest hardness. However, the hardness on the AS exhibited higher hardness than on the RS due to higher content of the SiC particles. Jariyaboon et al. [11] measured the peak temperature distribution during FSW of the 2024Al-T351 alloy. They found that the temperatures adjacent to the NZ were 480 ^{o}C. Liu et al. [12] found that the temperature of the HAZ reached up to 360-370 ^{o}C during FSW of 6061Al alloy. In this study, the MMC was welded after solution treatment. The temperature of the HAZ would reach up to the nucleation temperature of θ phase (Al_2Cu). The θ phase nucleated in the HAZ would inhibit the formation of GP zone in the natural aging process after welding. Therefore, the HAZ exhibited the lowest hardness. In the NZ, the distribution of the SiC particles was inhomogeneous and the volume fraction tended to increase from the RS to the AS. Therefore, the hardness of the NZ increased from

the RS to the AS. The hardness profile of the OS sample was almost similar to the NOS sample, indicating that the heat input of both the samples was similar in the welding process. It is noted that the hardness of the NZ on the AS for the NOS sample is slightly higher than that for the OS sample. This might be associated with higher content of SiC particles in the NOS sample.

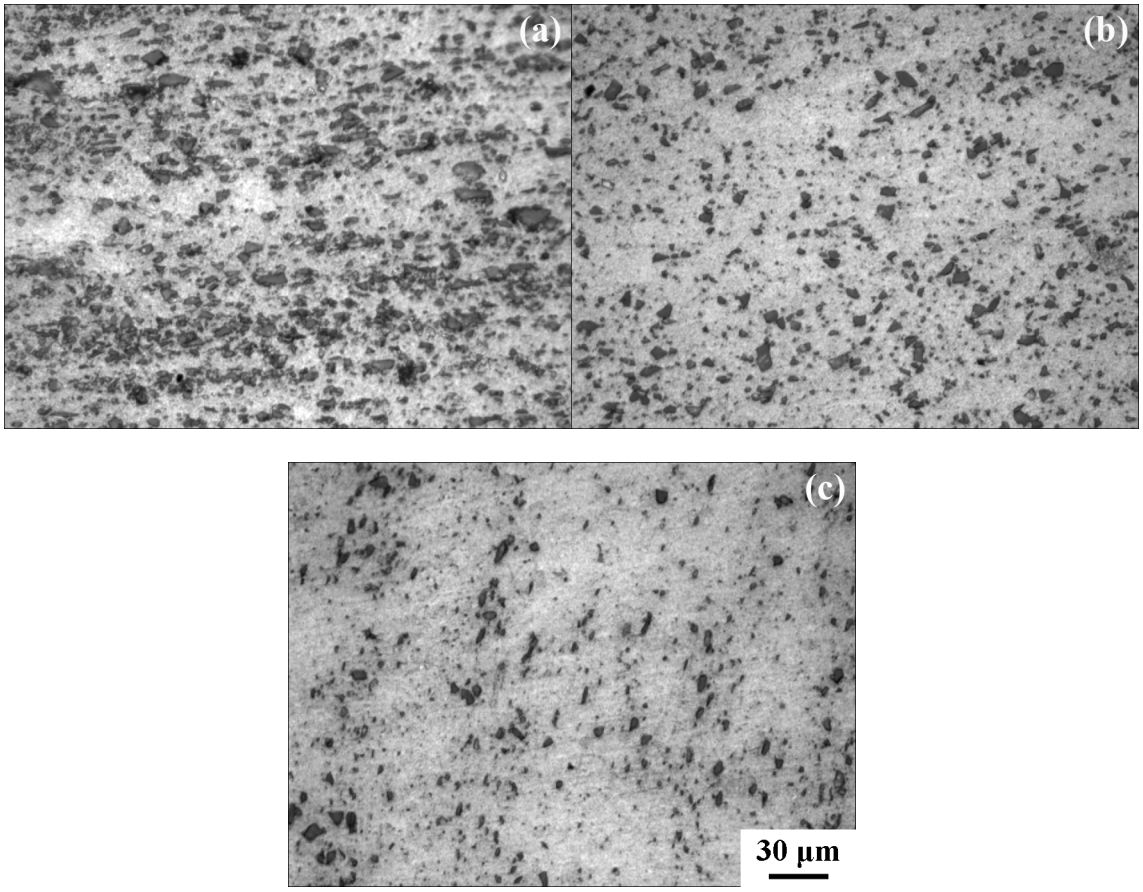

Figure 2. Optical micrographs showing SiC particle distribution in (a) SiC/2009, (b) NZ of NOS sample, and (c) NZ of OS sample.

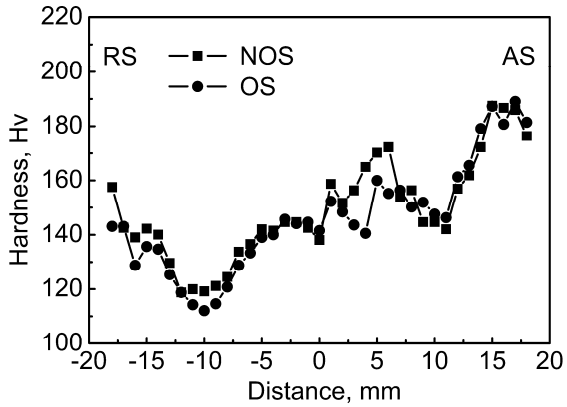

Figure 3. Hardness profiles of FSW MMC-2024Al joint.

The ultimate tensile strength (UTS) of the NOS sample is 387 MPa and reaches up to 85% of the 2024Al BM. The joint efficiency is similar to the FSW 2024Al joint [13]. The joint failed in the HAZ on the retreating (2024Al) side. However, the UTS of the OS sample is 214 MPa, only 47% of the 2024Al BM. Different from the NOS sample, the OS sample fractured along the edge of the NZ on the retreating side of the NZ. No fracture between the interface of MMC and 2024 Al alloy was observed, indicating that excellent bonding strength between them for both the NOS and OS

samples. However, different from the FSW 2024Al alloy joint, the OS sample did not failed in the HAZ, i.e. the lowest hardness regions. This implies that some other factors affected the strength of the OS samples.

Fig. 4a shows the SEM macrograph of the tensile fracture surface of the NOS sample and Fig. 4b shows the magnified view of the fracture surface. The fracture surface was characterized by small dimples showing the characteristic of shear fracture. The NOS tensile sample failed 45^{o}C to the tensile direction, which also suggested that the main mechanism of the fracture was the shear fracture. This was similar to that for the FSW 2000 series alloys [14]. Fig. 4c illustrated the macrograph of the fracture surface of the OS sample. The top of the surface consisted of the some dimples which is similar to the NOS sample. However, in the middle and bottom of the fracture surface very large dimples were observed. Fig. 4d shows the magnified views of the middle zone of the fracture surface. The large dimples showed the characteristic of plastic fracture. For the OS sample, the Al-clad layer of 2024Al plate was aggregated on the retreating side of the NZ and formed an Al layer along the edge of the NZ on the retreating side. The Al layer had a very low strength. In this case, the Al layer fractured firstly, when the sample was subjected to tension perpendicular to the welding direction. Therefore, the strength of the OS sample was lower than the 2024Al BM. Since the Al layer at the edge of the NZ was not extended to the top of the weld, the top of the fracture surface was similar to the NOS sample.

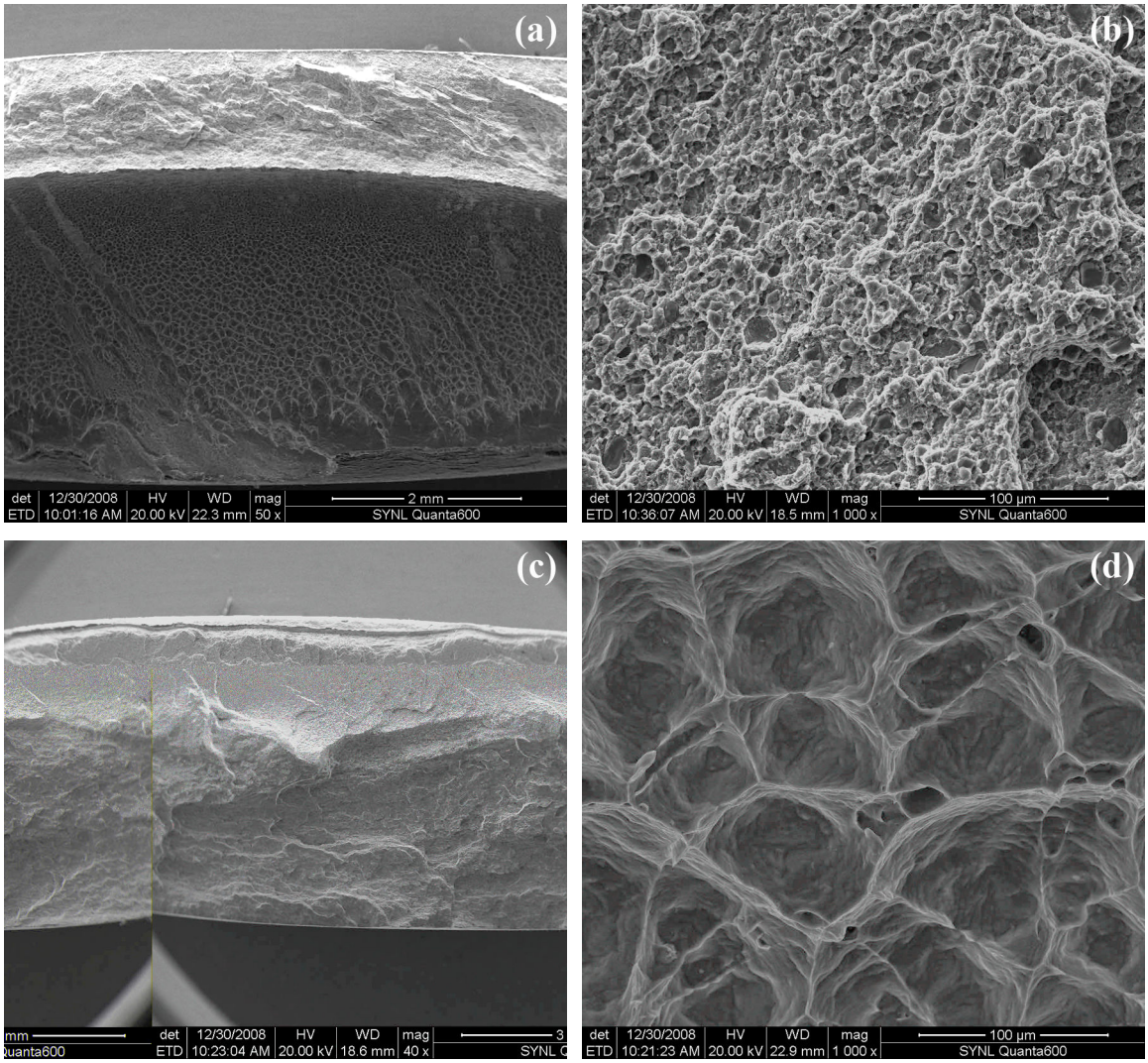

Figure 4. SEM image showing tensile fracture surfaces of FSW joint: (a), (b) NOS sample, (c), (b) OS sample.

Conclusions

1. Defect-free FSW 15vol.%SiCp/2009Al MMC and 2024Al-T351 alloy joint was successfully achieved with and without the tool pin offset to the 2024Al side.
2. The alternate distribution of the SiC particle-rich and -deficiency bands produced macrographically visible ring structure in the NZ. The Al-clad layer of the 2024Al alloy was aggregated at the edge of the nugget on the retreating side.
3. The strength of the NOS samples reached up to 85% of the 2024Al-T351 with the joint failing in the HAZ on the 2024Al side. The strength of the OS sample was only 47% of the 2024Al BM due to the aggregated Al layer on the retreating side.

Acknowledgments

This work was supported by the National Outstanding Young Scientist Foundation under Grant No. 50525103 and the Hundred Talents Program of Chinese Academy of Sciences.

Reference

[1] D. Storjohann, O.M. Barabash, S.S. Babu, S.A. David, P.S. Sklad, E.E. Bloom: Metall. Mater. Trans. Vol. 36A (2005), p. 3237

[2] R.S. Mishra, Z.Y. Ma: Mater. Sci. Eng. R vol. 50 (2005), p. 1

[3] A.H. Feng, B.L. Xiao, Z.Y. Ma: Compos. Sci. Technol. Vol. 68 (2008), p. 2141

[4] L.M. Marzoli, A.V. Strombeck, J.F. Dos Santos, C. Gambaro, L.M. Volpone, Compos. Sci. Technol. Vol. 66 (2006), p. 363

[5] L. Ceschini, I. Boromei, G. Minak, A. Morri, F. Tarterini: Compos. Sci. Technol. Vol. 67 (2007), p. 605

[6] J.A. Wert: Scripta Mater. Vol. 49 (2003), p. 607

[7] U. Fuchs, K. Zimmermann, H. W. Sauer, K.H. Trautmann1, G. Biallas: Mat.-wiss. u. Werkstofftech, Vol. 39 (2008), p. 531 (in German)

[8] Z.W. Chen, S. Cui: Scripta Mater. Vol. 58 (2008), p. 417

[9] P.B. Prangnell, C.P. Heason: Acta. Mater. Vol. 53 (2005), p. 3179

[10] C. Genevois, A. Deschamps, A. Denquin, B. Doisneau-cottignies: Acta. Mater. Vol. 53 (2005), p. 2447

[11] M. Jariyaboon, A.J. Davenport, R. Ambat, B.J. Connolly, S.W. Williams, D.A. Price: Corros. Sci. Vol. 49 (2007), p. 877

[12] F.C. Liu, Z.Y. Ma: Metall. Trans. Vol. 39A (2008), p. 2378

[13] C. Genevois, A. Deschamps, P. Vacher: Mater. Sci. Eng. Vol. 415 A (2006), p. 162

[14] P. Cavaliere, P.P. De Marco: Mater. Sci. Eng. Vol. 462 A (2007), p. 206

THERMEC 2009
10.4028/www.scientific.net/MSF.638-642

Friction Stir Welding of SiCp/Al Composite and 2024 Al Alloy
10.4028/www.scientific.net/MSF.638-642.1500

DOI References
[1] D. Storjohann, O.M. Barabash, S.S. Babu, S.A. David, P.S. Sklad, E.E. Bloom: Metall. Mater. Trans. Vol. 36A (2005), p. 3237
doi:10.1007/s11661-005-0093-4
[4] L.M. Marzoli, A.V. Strombeck, J.F. Dos Santos, C. Gambaro, L.M. Volpone, Compos. Sci. Technol. Vol. 66 (2006), p. 363
doi:10.1016/j.compscitech.2005.04.048
[5] L. Ceschini, I. Boromei, G. Minak, A. Morri, F. Tarterini: Compos. Sci. Technol. Vol. 67 (2007), p. 605
doi:10.1016/j.compscitech.2006.07.029
[7] U. Fuchs, K. Zimmermann, H. W. Sauer, K.H. Trautmann1, G. Biallas: Mat.-wiss. u. Werkstofftech, Vol. 39 (2008), p. 531 (in German)
doi:10.1002/mawe.200800317
[10] C. Genevois, A. Deschamps, A. Denquin, B. Doisneau-cottignies: Acta. Mater. Vol. 53 (2005), p. 2447
doi:10.1016/j.actamat.2005.02.007
[11] M. Jariyaboon, A.J. Davenport, R. Ambat, B.J. Connolly, S.W. Williams, D.A. Price: Corros. Sci. Vol. 49 (2007), p. 877
doi:10.1016/j.corsci.2006.05.038
[1] D. Storjohann, O.M. Barabash, S.S. Babu, S.A. David, P.S. Sklad, E.E. Bloom: Metall. Mater. rans. Vol. 36A (2005), p. 3237
doi:10.1007/s11661-005-0093-4
[4] L.M. Marzoli, A.V. Strombeck, J.F. Dos Santos, C. Gambaro, L.M. Volpone, Compos. Sci. echnol. Vol. 66 (2006), p. 363
doi:10.1016/j.compscitech.2005.04.048
[5] L. Ceschini, I. Boromei, G. Minak, A. Morri, F. Tarterini: Compos. Sci. Technol. Vol. 67 (2007), . 605
doi:10.1016/j.compscitech.2006.07.029
[6] J.A. Wert: Scripta Mater. Vol. 49 (2003), p. 607
doi:10.1016/S1359-6462(03)00215-X
[7] U. Fuchs, K. Zimmermann, H. W. Sauer, K.H. Trautmann1, G. Biallas: Mat.-wiss. u. erkstofftech, Vol. 39 (2008), p. 531 (in German)
doi:10.1002/mawe.200800317
[9] P.B. Prangnell, C.P. Heason: Acta. Mater. Vol. 53 (2005), p. 3179
doi:10.1016/j.actamat.2005.03.044
[10] C. Genevois, A. Deschamps, A. Denquin, B. Doisneau-cottignies: Acta. Mater. Vol. 53 (2005), . 2447
doi:10.1016/j.actamat.2005.02.007
[12] F.C. Liu, Z.Y. Ma: Metall. Trans. Vol. 39A (2008), p. 2378
doi:10.1007/s11661-008-9586-2
[13] C. Genevois, A. Deschamps, P. Vacher: Mater. Sci. Eng. Vol. 415 A (2006), p. 162
doi:10.1016/j.msea.2005.09.032
[14] P. Cavaliere, P.P. De Marco: Mater. Sci. Eng. Vol. 462 A (2007), p. 206

doi:10.1016/j.msea.2006.04.159